2010

HC-290 (Propane) Vaporisation Inside a Brazed Plate Heat Exchanger

Giovanni A. Longo
University of Padova - Dept. of Management and Engineering

HC-290 (Propane) Vaporisation Inside a Brazed Plate Heat Exchanger

Giovanni A. LONGO

University of Padova, Department of Management and Engineering
Str.lla S. Nicola No. 3, I-36100 Vicenza, Italy
Phone: +39 0444 998726 Fax: +39 0444 998888 E-Mail: tony@gest.unipd.it

ABSTRACT

This paper presents the heat transfer coefficients measured during HC-290 (Propane) vaporisation inside a brazed plate heat exchanger: the effects of heat flux, saturation temperature (pressure) and outlet conditions are investigated. The heat transfer coefficients show weak sensitivity to saturation temperature (pressure) and great sensitivity to heat flux and outlet conditions. The saturated boiling experimental heat transfer coefficients are compared with two well-known equations for nucleate boiling (Cooper (1984) and Gorenflo (1993)). The mean absolute percentage deviation between experimental and calculated heat transfer coefficients is 26.9% and 16.6% for Cooper (1984) and Gorenflo (1993) equation respectively. The heat transfer measurement has been complemented with IR thermography in order to quantify the portion of the heat transfer surface affected by vapour super-heating.

1. INTRODUCTION

All commonly used Hydro-Fluoro-Carbon (HFC) refrigerants have a high Global Warming Potential (GWP), higher than 1000, and some countries have already taken legislative measures towards a limitation in the use or a gradual phase-out of HFC. Hydro-Carbon (HC) refrigerants seem to be a real substitute for HFC refrigerants as they show good thermodynamic and transport properties, low GWP (< 100), high compatibility with traditional materials and mineral oils. HC refrigerants are already used in many applications such as domestic refrigeration, air conditioning, heat pump. HC-600a (Isobutane) is the alternative for HFC-134a in domestic refrigerators and commercial drink coolers, whereas HC-290 (Propane) and HC-1270 (Propylene) are used in chillers and heat pumps.
The major drawback of HC refrigerants is the flammability. The first attempt to reduce the risk of HC refrigerant is to decrease the refrigerant charge. The use of the Brazed Plate Heat Exchangers (BPHE) instead of the traditional tubular heat exchangers as evaporators and condensers in chiller and heat pumps allows a consistent reduction of the refrigerant charge with no penalty in system performance.
In open literature, it is possible to find only limited experimental data on HC refrigerants condensation and vaporisation inside BPHE. Pelletier and Palm (1996) experimentally compared HC-290 to HCFC-22 in condensation and vaporisation inside two different type of BPHE in a domestic heat pump. Palmer et al. (2000) measured the average Nusselt number during flammable refrigerants (HC-290, HC-290/HC-600a (70/30 wt%), HFC-32/HFC-152a (50/50 wt%)) vaporisation and condensation inside a BPHE in presence of lubricant oil: non-dimensional heat transfer correlations were presented. Corberan et al. (2000) and Setaro and Boccardi (2000) compared HC-290 to HCFC-22 heat transfer and pressure drop performance in condensation and vaporisation inside BPHE in an air to water reversible heat pump. Thonon and Bontemps (2002) carried out experimental tests on condensation of pure hydrocarbons (HC-601, HC-600, HC-290) and mixtures of hydrocarbons (HC-600/HC-290 (28/72 wt%) and (49/51 wt%)) in a BPHE and proposed a new heat transfer correlation for condensation of pure fluid. Longo (2009) experimentally investigated the effects of saturation temperature, refrigerant mass flux and fluid properties on HC-refrigerants 600a, 290 and 1270 condensation inside a BPHE.
This paper investigates the effects of heat flux, refrigerant mass flux, saturation temperature (pressure) and outlet conditions on HC-290 (Propane) vaporisation inside a BPHE.

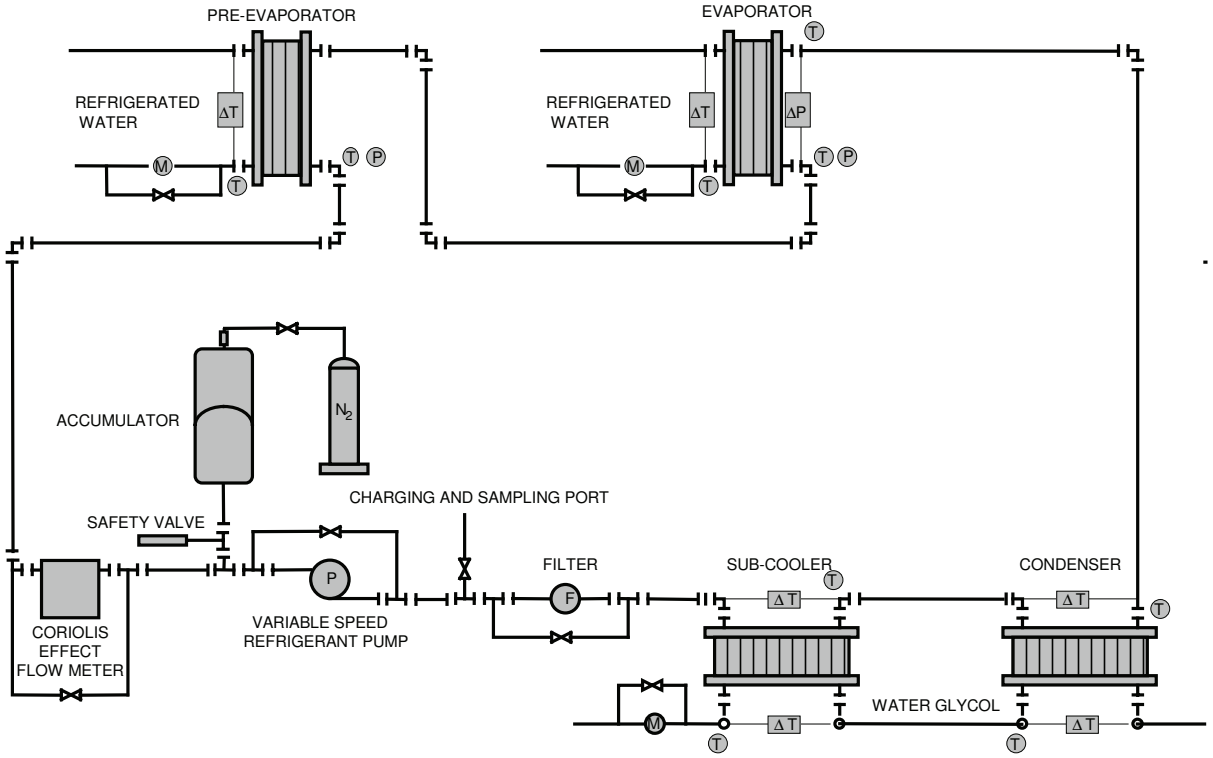

Figure 1: Schematic view of the experimental test rig

2. EXPERIMENTAL SET-UP AND PROCEDURES

The experimental facility, shown in figure 1, consists of a refrigerant loop, a water-glycol loop and a refrigerated water loop. In the first loop the refrigerant is pumped from the sub-cooler into the pre-evaporator where it is partially evaporated to achieve the set quality at the evaporator inlet. The refrigerant goes through the evaporator where it is evaporated and eventually super-heated and then it comes back to the condenser and the sub-cooler. A variable speed volumetric pump varies the refrigerant flow rate, whereas a bladder accumulator connected to a nitrogen bottle and a pressure regulator controls the operating pressure in the refrigerant loop. The second loop is able to supply a water-glycol flow at a constant temperature in the range of -10 to 30°C with a stability within ±0.1 K used to feed the sub-cooler and the condenser, whereas the third loop supplies a refrigerated water flow at a constant temperature in the range of 3 to 30°C with a stability within ±0.1 K used to feed the evaporator and the pre-evaporator. The evaporator is a BPHE consisting of 10 plates, 72 mm in width and 310 mm in length, which present a macro-scale herringbone corrugation with an inclination angle of 65° and a corrugation amplitude of 2 mm. Figure 2 and table 1 give the main geometrical characteristics of the BPHE tested. The temperatures of refrigerant and water at the inlet and outlet of the evaporator and the pre-evaporator are measured by T-type thermocouples (uncertainty (k= 2) within ±0.1 K), whereas water temperature drops through the evaporator and the pre-evaporator are measured by T-type thermopiles (uncertainty (k= 2) within ±0.05 K). The refrigerant pressures at the inlet of the evaporator and the pre-evaporator are measured by two absolute strain-gage pressure transducers (uncertainty (k= 2) within 0.075% f.s.), whereas the refrigerant pressure drop through the evaporator is measured by a strain-gage differential pressure transducer (uncertainty (k= 2) within 0.075% f.s.). The refrigerant mass flow rate is measured by means of a Coriolis effect mass flow meter (uncertainty (k= 2) of 0.1% of the measured value), whereas the water flow rates through the evaporator and the pre-evaporator are measured by means of magnetic flow meters (uncertainty (k= 2) of 0.15% of the f.s.). All the measurements are scanned by a data logger linked to a PC.

Prior to the start of each test the refrigerant is re-circulated through the circuit, the condenser and the sub-cooler are fed with water-glycol at a constant temperature and the evaporator and pre-evaporator are fed with water at a constant temperature. The refrigerant pressure and vapour quality at the inlet of the evaporator and the vapour quality or super-heating at the outlet of the evaporator are controlled by adjusting the bladder accumulator, the volumetric pump, the flow rate and the temperature of the water-glycol and the refrigerated water.

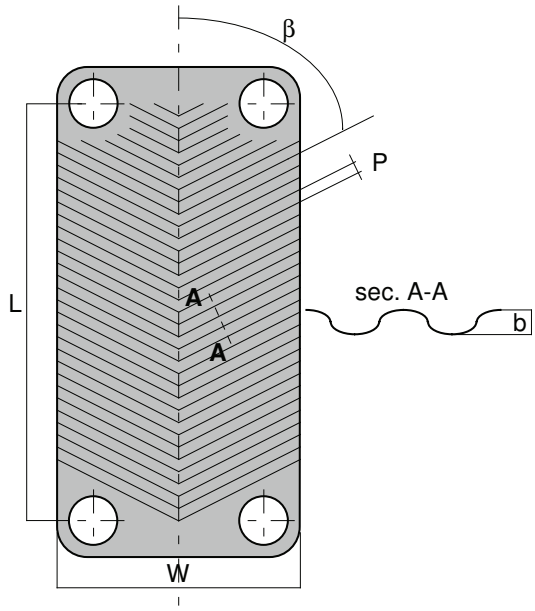

Figure 2: Schematic view of the plate

Table 1: Geometrical characteristics

Parameter	Measure / Type
Fluid flow plate length L (mm)	278.0
Plate width W(mm)	72.0
Area of the plate A(m^2)	0.020
Corrugation type	Herringbone
Angle of the corrugation β(°)	65
Corrugation amplitude b(mm)	2.0
Corrugation pitch P(mm)	8.0
Plate roughness R_a(μm)	0.4
Plate roughness R_p(μm)	1.0
Number of plates	10
Channels on refrigerant side	4
Channels on water side	5

Once temperature, pressure, flow rate and vapour quality steady state conditions are achieved at the evaporator inlet and outlet both on refrigerant and water sides all the readings are recorded for a set time and the average value during this time is computed for each parameter collected. The experimental results are reported in terms of refrigerant side heat transfer coefficients and frictional pressure drop.

3. DATA REDUCTION

The overall heat transfer coefficient in the evaporator U is equal to the ratio between the heat flow rate Q, the nominal heat transfer area S and the logarithmic mean temperature difference ΔT_{ln}

$$U = Q / (S\, \Delta T_{ln}) \tag{1}$$

The heat flow rate is derived from a thermal balance on the waterside of the evaporator:

$$Q = m_w\, c_{pw}\, |\Delta T_w| \tag{2}$$

where m_w is the water flow rate, c_{pw} the water specific heat capacity and $|\Delta T_w|$ the absolute value of the temperature variation on the water side of the evaporator.
The nominal heat transfer area of the evaporator

$$S = N\, A \tag{3}$$

is equal to the nominal projected area A = L × W of the single plate multiplied by the number N of the effective elements in heat transfer, as suggested by Shah and Focke (1988).
When the evaporator works only in two-phase heat transfer the logarithmic mean temperature difference is equal to:

$$\Delta T_{ln}=[(T_{wi}-T_{wo})/ln[(T_{wi}-T_{sat})/(T_{wo}-T_{sat})] \tag{4}$$

where T_{sat} is the average saturation temperature of the refrigerant derived from the average pressure measured on refrigerant side and T_{wi} and T_{wo} the water temperatures at the inlet and the outlet of the evaporator.
When the evaporator works both in vaporisation and super-heating, Dutto et al. (1991) and Fernando et al. (2004) suggested the following expression for the logarithmic mean temperature difference:

$$\Delta T_{ln}=Q/[(Q_{boil}/\Delta T_{ln.boil})+(Q_{sup}/\Delta T_{ln.sup})] \tag{5}$$

where

$$Q_{boil}=m_w c_{pw}(T_{wm}-T_{wo})] \tag{6}$$

$$Q_{sup}=m_w c_{pw}(T_{wi}-T_{wm})] \tag{7}$$

are the heat flow rate exchanged in the boiling and super-heating zones,

$$\Delta T_{ln.boil}=(T_{wm}-T_{wo})/ln[(T_{wm}-T_{sat})/(T_{wo}-T_{sat})] \quad (8)$$

$$\Delta T_{ln.sup}=[(T_{wi}-T_{rout})-(T_{wm}-T_{sat})] / ln[(T_{wi}-T_{rout})/(T_{wm}-T_{sat})] \quad (9)$$

is the logarithmic mean temperature difference in the boiling and super-heating zones, whereas T_{wm} is the water temperature between the super-heating and the boiling zone and T_{rout} is the refrigerant temperature at the outlet of the evaporator. The water temperature between the super-heating and the boiling zone is calculated from:

$$T_{wm} = T_{wi} - m_r\, c_{pGr}\, (T_{rout} - T_{sat}) / (m_w\, c_{pw}) \quad (10)$$

where m_r is the refrigerant flow rate and c_{pGr} is the specific heat capacity of the refrigerant vapour. This approach computes the overall heat transfer coefficient of the whole evaporator U as the average value between the overall heat transfer coefficient of the boiling zone U_{boil} and that of the super-heating zone U_{sup} weighted on the base of the respective heat transfer area.

The average heat transfer coefficient on the refrigerant side of the evaporator h_r is derived from the overall heat transfer coefficient U assuming no fouling resistances:

$$h_r = (1 / U - s / \lambda_p - 1 / h_w)^{-1} \quad (11)$$

by computing the waterside heat transfer coefficient h_w using a modified Wilson plot technique. A specific set of experimental water to water tests is carried out on the evaporator to determine the calibration correlation for heat transfer on the water side, in accordance with Muley and Manglik (1999); the detailed description of this procedure is reported by Longo and Gasparella (2007). The calibration correlation for water side heat transfer coefficient results:

$$h_w = 0.277\, (\lambda_w / d_h)\, Re_w^{0.766}\, Pr_w^{0.333} \quad (12)$$

The refrigerant vapour quality at the evaporator inlet and outlet X_{in} and X_{out} are computed starting from the refrigerant temperature $T_{pb.in}$ and pressure $p_{pb.in}$ at the inlet of the pre-evaporator (sub-cooled liquid condition) considering the heat flow rate exchanged in the pre-evaporator and in the evaporator Q_{pb} and Q and the pressure at the inlet and outlet p_{in} and p_{out} of the evaporator as follows:

$$X_{in} = f(J_{in}, p_{in}) \quad (13)$$

$$X_{out} = f(J_{out}, p_{out}) \quad (14)$$

$$J_{in} = J_{pb.in}(T_{pb.in}, p_{pb.in}) + Q_{pb} / m_r \quad (15)$$

$$J_{out} = J_{in} + Q / m_r \quad (16)$$

$$Q_{pb} = m_{pb.w}\, c_{pw}\, |\Delta T_{pb.w}| \quad (17)$$

where J is the specific enthalpy of the refrigerant, m_r the refrigerant mass flow rate, $m_{pb.w}$ the water flow rate and $|\Delta T|_{pb.w}$ the absolute value of the temperature variation on the water side of the pre-evaporator.

4. ANALYSIS OF THE RESULTS

A set of 61 vaporisation tests with refrigerant up-flow and water down-flow are carried out at three different saturation temperatures (10, 15 and 20°C) and four different evaporator outlet conditions (vapour quality around 0.80 and 1.00, vapour super-heating around 5 and 10°C), whereas the inlet vapour quality ranges between 0.22 and 0.36. Table 2 gives the main operating conditions in the evaporator under experimental tests: refrigerant saturation temperature T_{sat} and pressure p_{sat}, inlet and outlet refrigerant vapour quality X_{in} and X_{out}, outlet refrigerant super-heating ΔT_{sup}, mass flux on refrigerant side G_r and water side G_w, heat flux q. A detailed error analysis performed in accordance with Kline and McClintock (1953) indicates an overall uncertainty within ±12.0% for the refrigerant heat transfer coefficient measurement and within ±14.8% for the refrigerant total pressure drop measurement.

Figures 3, 4 and 5 show the average heat transfer coefficients on the refrigerant side against heat flux for three different saturation temperatures (10, 15 and 20°C) and four different evaporator outlet conditions (vapour quality around 0.80 and 1.00, vapour super-heating around 5 and 10°C).

Table 2: Operating conditions during experimental tests

Runs	T_{sat}(°C)	p_{sat}(MPa)	X_{in}	X_{out}	ΔT_{sup}(°C)	G_r(kg/m^{2}s)	G_w(kg/m^{2}s)	q(kW/m^2)
61	9.8–20.2	0.63–0.84	0.22–0.36	0.78–1.00	4.6–10.4	7.1–19.6	50.8–165.6	4.3–18.7

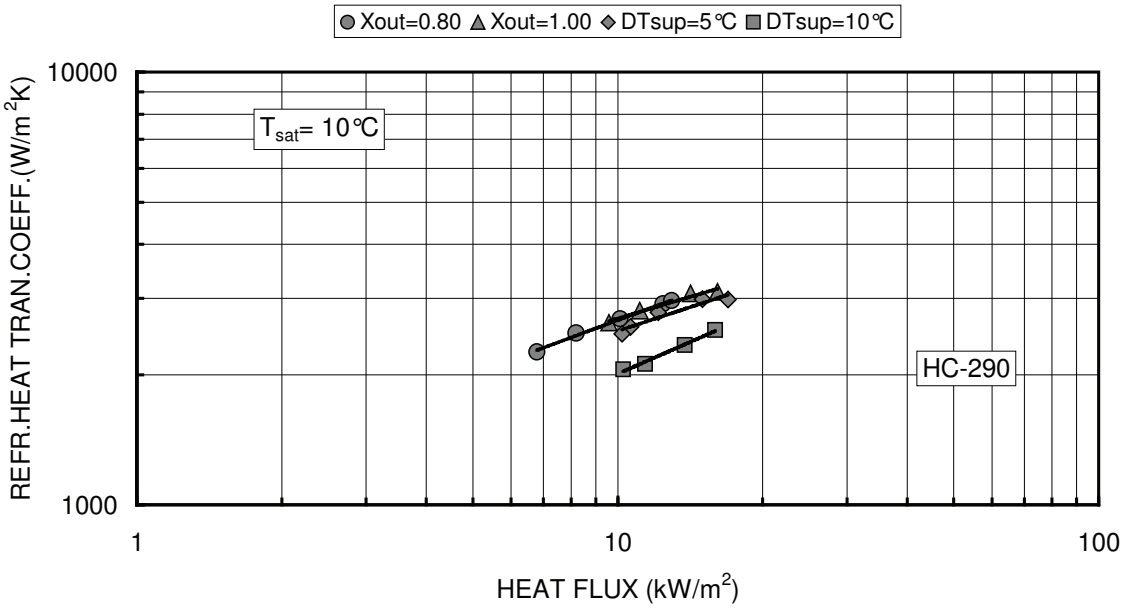

Figure 3: Average heat transfer coefficient on refrigerant side vs. heat flux at 10°C of saturation temperature

The heat transfer coefficients show great sensitivity to heat flux and outlet condition and weak sensitivity to saturation temperature (pressure). The saturated boiling heat transfer coefficients with an outlet vapour quality around 0.80 are from 0 to 2% higher than the saturated boiling heat transfer coefficients with an outlet vapour quality around 1.00, 4-7% higher than the heat transfer coefficients with 5°C of outlet vapour super-heating and 20-35% higher than the heat transfer coefficients with 10°C of outlet vapour super-heating. The weak decrease of the heat transfer coefficient with increasing vapour quality is probably due to dry-out inception in the upper part of the evaporator. The marked decrease of the heat transfer coefficient with vapour super-heating is due to the increase in the super-heating portion of the heat transfer surface which is affected by gas single phase heat transfer coefficients one or two orders of magnitude lower than the two phase heat transfer coefficients in the boiling portion of the heat transfer surface.

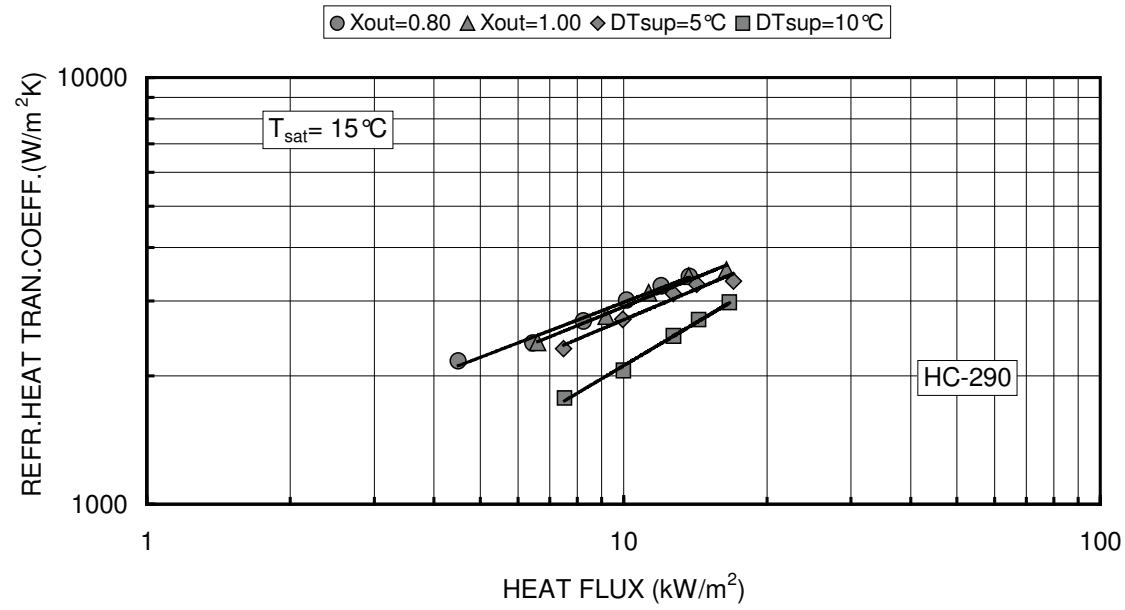

Figure 4: Average heat transfer coefficient on refrigerant side vs. heat flux at 15°C of saturation temperature

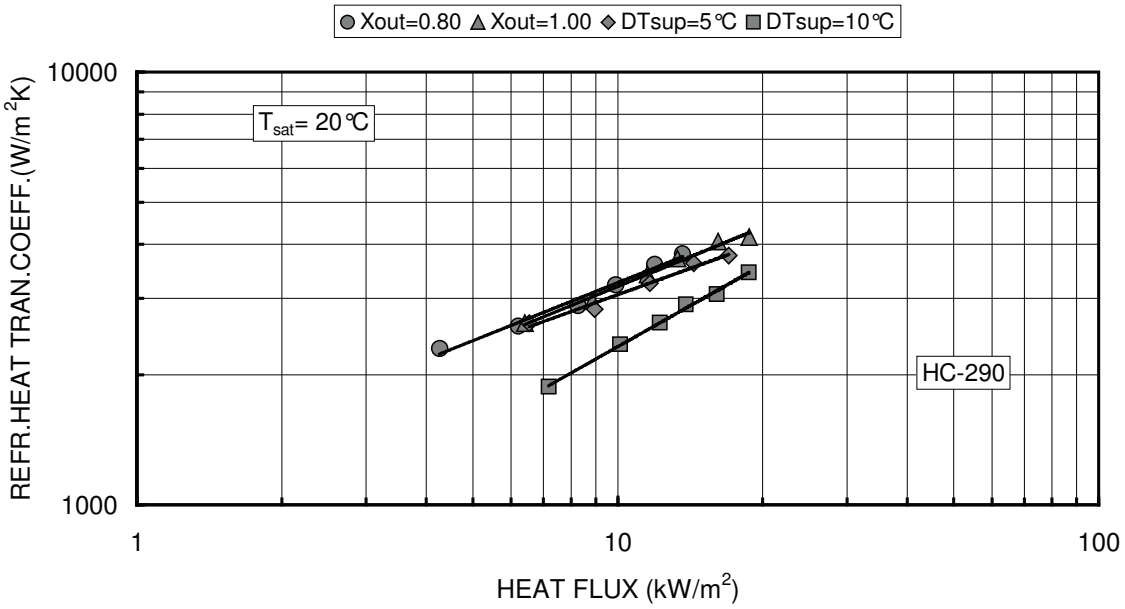

Figure 5: Average heat transfer coefficient on refrigerant side vs. heat flux at 20°C of saturation temperature

The saturated boiling experimental heat transfer coefficients ($X_{out} \leq 1$) are compared with two well-known correlations for nucleate boiling: Cooper (1984) and Gorenflo (1993) equations. Figures 6a and 6b show the comparison between experimental and calculated heat transfer coefficients by Cooper (1984) and by Gorenflo (1993) equations respectively. The mean absolute percentage deviations are 26.9% for Cooper (1984) equation and 16.2% for Gorenflo (1993) equation.

In order to quantify the portion of the heat transfer surface affected by vapour super-heating the flank of the BPHE has been filmed during the experimental tests by a IR thermo-camera (temperature uncertainty (k= 2) = ±0.1°C). Figure 7 shows the results of the IR thermography carried out during HC-290 vaporisation tests at 10°C of saturation temperature with a heat flux around 9-10 kW/m^2 and different evaporator outlet conditions: the dotted line indicates the BPHE profile.

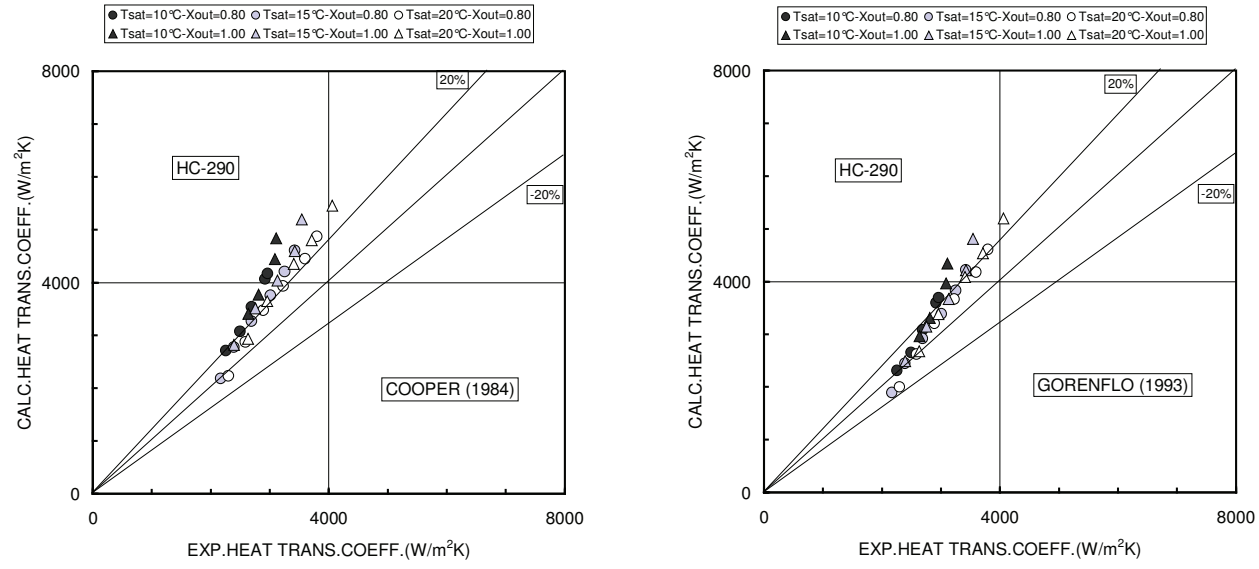

a) b)

Figure 6: Comparison between experimental and calculated heat transfer coefficient

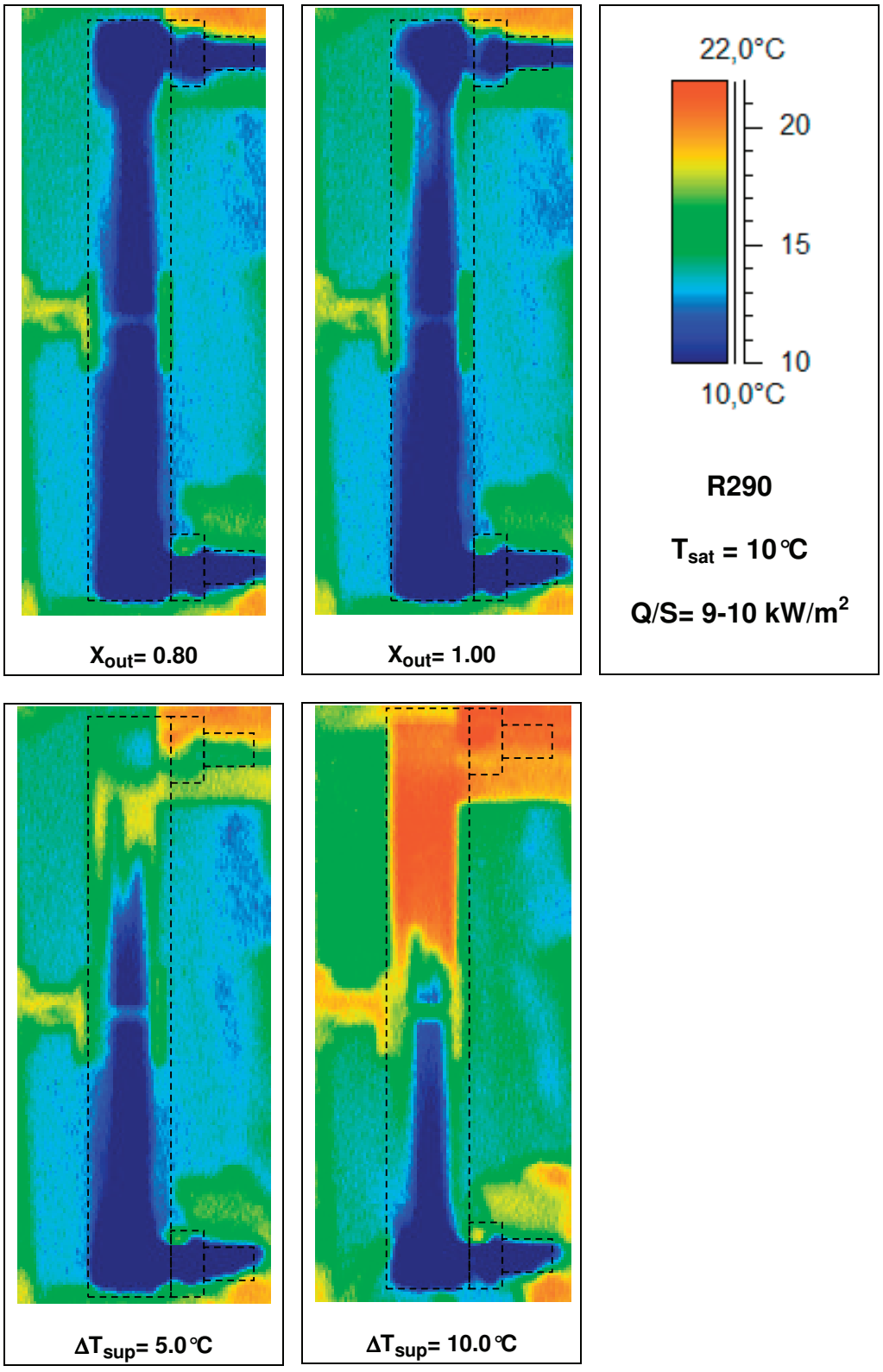

Figure 7: IR thermography of the BPHE during HC-290 vaporisation tests at 10°C of saturation temperature with a heat flux around 9-10 kW/m^2 and different evaporator outlet conditions

During the tests with saturated vapour outlet (X_{out} = 0.80 and 1.00) the whole heat transfer surface works in two-phase heat transfer and it is near to saturation temperature (blue colour). At 5°C of outlet vapour super-heating around 15-20% of the heat transfer surface (yellow-green area in the upper part of the BPHE) is affected by super-heating, whereas at 10°C of outlet vapour super-heating this portion increases up to 35-40% (red area in the upper part of the BPHE).

5. CONCLUSIONS

This paper investigates the effect of heat flux, saturation temperature (pressure) and outlet conditions on HC-290 heat transfer vaporisation inside a BPHE.

The heat transfer coefficients show weak sensitivity to saturation temperature (pressure) and great sensitivity to heat flux and outlet conditions. The saturated boiling heat transfer coefficients are 20-35% higher than those with 10°C of outlet vapour super-heating. The IR thermography shows that at 10°C of outlet vapour super-heating around 35-40% of the heat transfer surface is affected by super-heating,

Cooper (1984) and Gorenflo (1993) correlations are able to reproduce sufficiently well saturated boiling heat transfer coefficients.

REFERENCES

Cooper, M.G., 1984, Heat flows rates in saturated pool boiling – A wide ranging examination using reduced properties, in *Advanced in Heat Transfer*, Academic Press, Orlando, Florida, p.157-239.

Corberan, J., Urcheguia, J., Gonzalvez, J., Setaro, T., Boccardi G., and Palm, B., 2000, Two-phase heat transfer in brazed plate heat exchangers evaporators and condensers for R22 and propane, *Proc. 3rd European Thermal Science Conference,* p. 1193-1198.

Dutto, T. , Blaise, J.C., and Benedic, T., 1991, Performances of brazed plate heat exchanger set in heat pump, *Proc 18th Int. Congr. Refrigeration*, Montreal, Canada, p. 1284-1288.

Fernando, P., Palm, B., Lundqvist, P., and Granryd, E., 2004, Propane heat pump with low refrigerant charge: design and laboratory tests, *Int. J. Refrigeration*, vol.27, p. 761-773.

Gorenflo, D., 1993, Pool boiling, in *VDI Heat Atlas*, Dusseldorf, Germany, p. Ha1-25.

Kline, S.J., and McClintock, F.A., 1953, Describing uncertainties in single-sample experiments, *Mech.Eng*., vol.75, p. 3-8.

Longo, G.A., and Gasparella, A., 2007, Heat transfer and pressure drop during HFC refrigerant vaporisation inside a brazed plate heat exchanger, *Int. J. of Heat Mass Transfer*, vol.50, p. 5194-5203.

Longo. G.A., 2009, Heat transfer and pressure drop during hydrocarbon refrigerant condensation inside a brazed plate heat exchanger," *Proc 3rd IIR Conference on Thermophysical Properties and Transport Processes of Refrigerants*, Boulder, CO, USA

Muley, A., and Manglik, R.M., 1999, Experimental study of turbulent flow heat transfer and pressure drop in a plate heat exchanger with chevron plates, *ASME J. Heat Transfer*, vol.121, p. 110-121.

NIST, 2002, Refrigerant properties computer code, REFPROP 7.0.

Palmer, S.C., Vance Payne,W., and Domanski, P.A., 2000, Evaporation and condensation heat transfer performance of flammable refrigerants in a brazed plate heat exchanger, NIST, IR 6541.

Pelletier, O., and Palm, B., 1996, Performance of plate heat exchangers and compressor in a domestic heat pump using propane, *Proc. Aarhus Conf.,* IIF/IIR, p.497-505.

Setaro, T., and Boccardi, G., 2000, Comparative study of evaporation and condensation of propane and R22 in a brazed plate heat exchanger and tube-fin coil, *Proc. 4th IIR Gustav Lorentzen Conf*., Purdue, IN, USA, p. 242-247.

Shah, R.K., and Focke, W.W., 1988, Plate heat exchangers and their design theory, in *Heat Transfer Equipment Design*, Hemisphere, Washington, p.227-254.

Thonon, B., and Bontemps, A., 2002, Condensation of pure and mixture of hydrocarbons in a compact heat exchanger: experiments and modelling, *Heat Transfer Eng*., vol.23, p. 3-17.